CHAPTER VI

TROPICAL ATMOSPHERE BOUNDARY LAYER: MODELLING THE GROWTH OF THE MIXING LAYER USING A CONVENTIONAL SLAB MODEL

6.1 INTRODUCTION

The daytime convective boundary layer (CBL) plays an important role in the land-surface atmosphere interaction by controlling the transfer of the turbulent fluxes from the surface to the free atmosphere. Following the breakdown of the stably stratified nocturnal boundary layer in the morning, a shallow CBL forms that gradually increases in depth during the day because the surface fluxes (both thermal and mechanical) provide energy that allows air parcels to rise, overshoot the top of the inversion, and then return (due to continuity), thereby entraining warm and dry air from aloft into the layer. The CBL does not merely grow in response to this turbulence but has mechanisms of interaction operating in the opposite direction: the entrainment flux brings drier air into the layer, thereby changing the saturation deficit and hence modifying the partition of energy in terms of sensible and latent heat fluxes at the surface (Fisch, 1996).

The CBL height is one of the scaling parameters that describes the processes of the planetary boundary layer (PBL) and is an important parameter in environmental meteorology. Therefore the computed/observed CBL height could be used for validating the PBL parameterisation in mesoscale models and also in estimating the dispersion of the contaminants in air pollution models. As shown in the review in Chapter III, the CBL height (the mixing layer height) can be estimated from measurements performed by radiosonde, sodars, and lidars. Recent investigations have shown the ability of windprofiles/RASS systems to measure vertical temperatures accurately. The CBL height can also be estimated by numerical one-dimensional (1-D), two-dimensional (2-D), and three-dimensional (3-D) models. In general, 2-D and 3-D boundary layer modelling approaches have been found to be superior for simulating the processes of the ABL and for predicting the CBL heights. However, under certain conditions, a 1-D model has been found to be economical and to provide a realistic simulation of the PBL. Furthermore, 1-D models can be applied at locations where only single point data are available (Nagar *et al.*, 2001). Simple 1-D models for the vertical structure of the PBL are used in climatological data analysis (Martano & Romanelli, 1997).

Tennekes (1973) was the first to model the growth of the ABL in the presence of free or forced convection (unstable atmosphere), i.e., under diurnal conditions. In his classic article, Tennekes idealised the ABL as being composed of a well mixed layer in which the thermodynamic properties (potential temperature) are constant with height. At the top of the layer, there is a discontinuity followed by a thermal inversion (Fisch, 1996), referred to as the mixing layer. The turbulence within this layer is maintained primarily by convection and wind shear. The so called "encroachment" models (Carson

& Smith, 1974) deal only with the thermodynamics and neglect turbulent entrainment. The encroachment equation for the height of the mixed layer is derived from the budget of heat energy (Panofsky & Dutton, 1984). Entrainment of warm air aloft is assumed to be absent, and consequently there is no temperature difference across the top of the mixed layer. A review of the major developments in approaches to modelling the growth of the mixing layer, and indeed the mixing height, has been presented in Chapter III.

The CBL in the tropics has to be well understood and accurately represented in air pollution dispersion models. The objective of this work is to examine the ability of the conventional slab models to simulate the evolution and the structure of the daytime boundary layer in the tropics, based on the theory developed by Tennekes (1973) and the model developed by Batchvarova & Gryning (1991, 1994). Their simplified model for the mixing layer takes into account the temperature differences across the top of the layer and includes the effect of convective and mechanical turbulence as well as the spin-up in the entrainment process. The model enables the derivation of approximate solutions that are still sufficiently complex to retain the basic physical parameters. Detailed observations on the tropical boundary layer growth and surface forcings, presented in Chapter IV and Chapter V, are used to verify these estimates.

6.2 THE MODEL

The model used in this thesis can be visualised as a single layer box. The box grows in height due to the input of energy from the bottom, forced by surface fluxes, and from the top due to entrainment flux, which includes contributions from both thermally and

mechanically generated turbulence. In the idealized model adopted here, the air inside the box is well mixed with a uniform profile of virtual potential temperature within the mixed layer (Carson, 1973; Tennekes, 1973; Fisch *et al.* 1996). The entrainment zone is represented by an infinitesimally thin inversion. The air above the mixed layer is stably stratified. The model assumes horizontal homogeneity, neglects direct heating of the air from radiation, and accounts for latent heat effects by applying the virtual potential temperature. Generally, the assumption of uniform potential temperature in the mixed layer is in accordance with measurements, whereas the representation of the entrainment zone is highly idealised in this model (Batchvarova & Gryning, 1991). The model has been studied under different atmospheric conditions and types of surface by several researchers (e.g., Tennekes, 1973; Driedonks, 1981; McNaughton & Spriggs, 1986; Batchvarova & Gryning, 1991, Gryning & Batchvarova, 1990a; Culf, 1992; Fisch *et al.*, 1996).

The model suggests a boundary layer capped by the so-called entrainment zone, a layer of strong stratification. It is confined between the height reached by only the most vigorous turbulent eddies and the height below which the boundary layer is not intermittent. The physical basis of the model is shown schematically in Figure 3.1 b. Above the boundary layer, air is stably stratified with a potential temperature gradient independent of height and time. Inside the internal boundary layer, turbulence is assumed to maintain a uniform vertical distribution of potential temperature. The finite inversion, which caps the layer, is assumed to be infinitesimally thin.

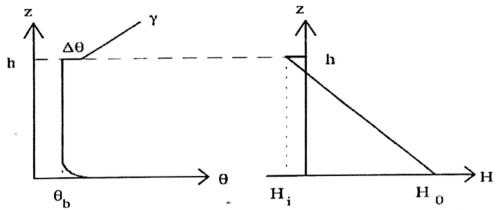

Figure 6.1: Schematic illustration of the physical system that forms the basis of the model (H_i: sensible flux at the inversion height $\left(\overline{\omega'\theta'}\right)_h$ and H_o: sensible heat flux at the surface $\left(\overline{\omega'\theta'}\right)_s$).

In the following sub-sections, a theoretical background of the convective slab model is presented in detail, based on the work by Gryning & Batchvarova (1990) and Batchvarova & Gryning (1991).

6.2.1 Turbulent Kinetic Energy

As the boundary layer grows, warm air from the overlying free flow is entrained into it and the entrained air must adjust to the level of the turbulent kinetic energy inside the boundary layer. Because the air in the overlying free flow is warmer than the air within the boundary layer, and the turbulent kinetic energy is lower, both processes consume energy. The required energy is supplied from the turbulent kinetic energy within the boundary layer, which limits the entrainment rate. Thus, the mixed layer entrains at a rate that is partly determined by the production of turbulent kinetic energy within the

boundary layer, and partly by the amount of the turbulent kinetic energy that is available for entrainment processes.

The production of the turbulent kinetic energy within the boundary layer is the controlling influence on the entrainment velocity. The equation for the mean turbulent kinetic energy (TKE) may be written as:

$$\frac{d\overline{e'}}{dt} = -\overline{u'w'}\frac{d\bar{u}}{d\bar{z}} + \frac{g}{\bar{\theta}}\overline{\theta'\omega'} - \frac{d\left(\overline{e\omega'}\right)}{dz} - \frac{\hat{1}}{\rho}\frac{d\left(\overline{p'\omega'}\right)}{dz} - \varepsilon \qquad (6.1)$$

where e is the turbulent kinetic energy; $-\overline{u'w'}$ is the momentum flux; $\overline{\theta'\omega'}$ is the kinetic heat flux; $\left(\overline{e'\omega'}\right)$ is the flux of turbulent kinetic energy; $\left(\overline{p'\omega'}\right)$ is the redistribution by pressure perturbations; ε is viscous dissipation; θ_v is virtual temperature; and g is the acceleration due to gravity. Over-bars indicate mean values and primes indicate perturbation components. Integration of Equation 6.1 across the depth of the boundary layer and the inversion yields:

$$\int_0^h \frac{d\overline{e'}}{dt}dz = -\int_0^h \overline{u'w'}\frac{d\bar{u}}{d\bar{z}}dz + \frac{g}{\bar{\theta}}\int_0^h \overline{\theta'\omega'}dz - \int_0^h \frac{d\left(\overline{e\omega'}\right)}{dz}dz - \frac{1}{\rho}\int_0^h \frac{d\left(\overline{p'\omega'}\right)}{dz}dz - \int_0^h \varepsilon dz \qquad (6.2)$$

which can be rewritten as:

$$\frac{d}{dt}\int_0^h \overline{e'}dz + \overline{e'_h}\frac{dh}{dt} = -\int_0^{h-\delta} \overline{u'w'}\frac{d\overline{u}}{dz}dz - \int_{h-\delta}^{h} \overline{u'w'}\frac{d\overline{u}}{dz}dz + \frac{g}{\overline{\theta}}\int_0^h \overline{\theta'\omega'}dz - \left(\overline{e\omega'}\right)_h + \left(\overline{e\omega'}\right)_s$$

$$-\frac{1}{\rho}\left(\overline{p'\omega'}\right)_h + \frac{1}{\rho}\left(\overline{p'\omega'}\right)_s - \int_0^h \varepsilon dz \qquad (6.3)$$

where the thickness δ is introduced in order to account for the jump conditions across the inversion. Equation 6.3 is clearly not in a form suitable for applied use, hence the various terms need to be parameterised in terms of measurable flow quantities or shown to be insignificant. A considerable literature exists on this issue, and the parameterisation of the various terms is briefly presented as follows:

$\frac{d}{dt}\int_0^h \overline{e'}dz$: Change with time of the total TKE; negligible (Mahrt & Lenschow, 1976).

$\overline{e'_h}\frac{dh}{dt}$: Parameterised as $C u_*^2 \frac{dh}{dt}$ (Zilitinkevich, 1975); the so-called spin-up term that accounts for the energy needed to bring the newly entrained air just below the inversion to the quasi-equilibrium TKE-level of the boundary layer.

$-\int_0^{h-\delta} \overline{u'w'}\frac{d\bar{u}}{dz}dz$: Parameterised as Bu_*^3 (Tennekes, 1973); mechanical production of TKE within the boundary layer.

$-\int_{h-\delta}^{h} \overline{u'w'}\frac{d\bar{u}}{dz}dz$: $\left(\Delta u^2 + \Delta v^2\right)\frac{dh}{dt}$ where Δu and Δv are the wind velocity changes in the u-direction and v-direction across the inversion. The term is generally considered to be small (Mahrt & Lenschow, 1976); however, Manins (1982) claimed it to be important. The term accounts for mechanical production of TKE caused by the jump in wind velocity across the inversion.

$\frac{g}{\bar{\theta}}\int_0^h \overline{\theta'\omega'}dz$: Parameterises as $\frac{gh}{2\bar{\theta}}\left[\left(\overline{\omega'\theta'}\right)_h + \left(\overline{\omega'\theta'}\right)_s\right]$. The profile of $\left(\overline{\omega'\theta'}\right)$ is shown in the right panel of Figure 6.1. Formally it is split into two parts where $\frac{gh}{2\bar{\theta}}\left(\overline{\omega'\theta'}\right)_s$ is the buoyancy production of TKE, and $\frac{gh}{2\bar{\theta}}\left(\overline{\omega'\theta'}\right)_h$ is the energy expended to do the work necessary to bring the entrained air down.

$\left(\overline{e\omega'}\right)_h + \left(\overline{e\omega'}\right)_s$: negligible (Stull, 1976a); $\left(\overline{e\omega'}\right)$ describes the turbulent transport of TKE in the boundary layer. The integrated transport term is negligible

because there is no transport to the non-turbulent free flow, $\left(\overline{e\omega'}\right)_h$, or to the ground $\left(\overline{e\omega'}\right)_s$.

$-\frac{1}{\rho}\left(\overline{p'\omega'}\right)_h$: usually neglected, $\left(\overline{p'\omega'}\right)$ describes how TKE is redistributed by pressure fluctuations inside the boundary layer. $\left(\overline{p'\omega'}\right)_h$ is related to gravity waves draining energy from the top of the boundary layer, (Mahrt & Lenschow, 1976).

$\frac{1}{\rho}\left(\overline{p'\omega'}\right)_s$: negligible because the redistribution term vanishes at the ground (Stull, 1976a).

$-\int_0^h \varepsilon dz\, q$: roughly 98 % of the TKE generated is lost due to dissipation (Stull, 1976a). The available energy for the entrainment process is the very small difference between the large production and dissipation terms in Equation 6.2. Here the dissipation rate is considered to be proportional to the production rate, thus the dissipation term is absorbed in the parameterisation constants A and B.

6.2.2 Mixing Layer Equations

Here an expression of the inversion strength, Δ, is obtained as a function of h and atmospheric stability. Because warm air is entrained in the cooler boundary layer, the

heat flux at the top of the boundary layer is downward. Invoking the entrainment rate dh/dt, we have (Lilly, 1968):

$$- (\overline{\theta'\omega'})_h = \Delta \frac{dh}{dt} \tag{6.4}$$

where $- (\overline{\theta'\omega'})_h$ is the vertical kinematic heat flux at the top of the boundary layer and t is time. The inversion strength, Δ, will tend to increase due to entrainment of the boundary layer into stable air above. It will tend to decrease as the boundary layer is heated, because of entrainment of warm air from above and heating of the ground. Therefore,

$$\frac{d\Delta}{dt} = \gamma \frac{dh}{dt} - \left(\frac{d\bar{\theta}}{dt}\right)_{bl} \tag{6.5}$$

where γ is the potential temperature gradient above the layer, and $\left(\frac{d\bar{\theta}}{dt}\right)_{bl}$ is the heating rate of the air in the boundary layer. The heating rate is

$$\left(\frac{d\bar{\theta}}{dt}\right)_{bl} = \frac{\left(\overline{\omega'\theta'}\right)_s}{h} - \frac{\left(\overline{\omega'\theta'}\right)_h}{h} \tag{6.6}$$

where $\left(\overline{\omega'\theta'}\right)_s$ is the vertical kinematic heat flux at the surface.

6.2.3 Entrainment Hypothesis

To complete the set of equations, an expression is needed for the flux through the top of the mixed layer. A considerable literature exists to describe such an expression. The extra equation is usually obtained by integrating the budget of the TKE over the mixed layer.

Section 6.2.1 contains a review and discussion of the parameterisation and significance with respect to mixed layer growth of the terms in the budget for turbulent kinetic energy. By considering Equation 6.3 and neglecting the terms that are generally considered small or negligible in the literature, Gryning & Batchvarova (1991) arrived at the parameterised energy-budget:

$$-\frac{gh}{\overline{\theta}}(\overline{\theta'\omega'})_h + Cu_*^2\frac{dh}{dt} = A\frac{gh}{\overline{\theta}}(\overline{\theta'\omega'})_s + Bu_*^3 \qquad (6.7)$$

where g/T is the buoyancy parameter. The left hand side represents the consumption of the potential and kinetic energy at the inversion by the entrainment process, and the right hand side represents the main production terms of energy (TKE) within the boundary layer. A, B, and C are parameterisation constants.

The available energy for the entrainment process is sourced from the small difference between the production and dissipation of the turbulent kinetic energy. Gryning & Batchvarova (1990a) and Batchvarova & Gryning (1991, 1994) considered

the dissipation rate to be proportional to the production rate; thus the effect of dissipation is absorbed in the parameterisation constants A and B.

Solving for the downward directed heat flux at the inversion reads

$$-(\overline{\theta'\omega'})_h = A(\overline{\theta'\omega'})_s + \frac{Bu_*^3\bar{\theta}}{gh} - \frac{Cu_*^2\bar{\theta}}{gh}\frac{dh}{dt} \qquad (6.8)$$

where the last term on the right hand side represents the spin-up effect or Zilitinkevich correction (Zilitinkevich, 1975). Gryning & Batchvarova (1990b) showed that the spin-up term is important only when the boundary layer is shallow (50-100 m), or the free flow is near neutral stratified. These conditions have not been considered by some authors, and allows Equation. 6.8 to be written and used as:

$$-(\overline{\theta'\omega'})_h = A(\overline{\theta'\omega'})_s + \frac{Bu_*^3\bar{\theta}}{gh} \qquad (6.9)$$

For small values of h it follows from Equation 6.8 that:

$$\frac{dh}{dt} = \frac{B}{C}u_*$$

showing that the growth rate of a shallow mixed layer is proportional to the friction velocity. The spin-up term depends not only on u_* but also on the convective velocity

scale $w^* = (g/T)\ (\overline{\theta'\omega'})_s\, h)^{1/3}$ (Tennekes & Driedonks, 1981). The dependence on w^* has not been included because the spin-up term is important mainly in the morning where w^* is small.

The usual value of A is 0.2 (Tennekes, 1973; Stull, 1976a), and is a value now widely accepted. Based on laboratory experiments, Kato & Phillips (1969) reported B=2.5. The value of C was estimated as 8 (Zilitinkevich, 1975; Tennekes & Driedonks, 1982b). These values are used in this study.

6.2.4 Inversion Strength

The spin-up term will be neglected when deriving the expression for the temperature difference across the inversion. The term is insignificant when the mixed layer is shallow. In the context of mixed layer growth, the effect of the inversion is negligible under such conditions. Substituting Equations 6.4 and 6.6 into 6.5 yields:

$$\left(h\frac{d\Delta}{dh} + \Delta - \gamma h\right)\frac{dh}{dt} = -\left(\overline{\omega'\theta'}\right)_s \tag{6.10}$$

and then from Equation 6.4,

$$h\frac{d\Delta}{dh} + \Delta - \gamma h = -\Delta\frac{\left(\overline{\omega'\theta'}\right)_s}{A\left(\overline{\omega'\theta'}\right)_s + \dfrac{Bu_*^3 T}{gh}} \tag{6.11}$$

By introducing the Obukhov length,

$$L = -\frac{u_*^3 \bar{\theta}}{\kappa g \left(\overline{\omega'\theta'}\right)_s} \tag{6.12}$$

Where κ is the von Karman constant, Equation 6.11 can be rewritten as:

$$\frac{d\Delta}{dh} + \Delta\left(\frac{1}{h} + \frac{1}{Ah - B\kappa L}\right) = \gamma \tag{6.13}$$

Equation 6.13 is an ordinary linear first-order differential equation; the solution is

$$\frac{\Delta}{\gamma h} = \frac{\dfrac{1}{1+2A}\left(\dfrac{1}{Ah - B\kappa L}\right)^{\frac{1+2A}{A}} + \dfrac{B\kappa L}{1+A}\left(Ah - B\kappa L\right)^{\frac{1+A}{A}}}{Ah^2\left(Ah - B\kappa L\right)^{1/A}} + \frac{\left(-B\kappa L\right)^{\frac{1+2A}{A}}\left(\dfrac{1}{1+A} - \dfrac{1}{1+2A}\right)}{Ah^2\left(Ah - B\kappa L\right)^{1/A}} \tag{6.14}$$

where the integration constant was chosen so that Equation 6.14 always remains finite:

$$\frac{\Delta}{\gamma h} = \frac{1}{2} \qquad \text{for } \frac{h}{L} \to -0 \tag{6.15}$$

$$\frac{\Delta}{\gamma h} = \frac{A}{1+2A} \qquad \text{for } \frac{h}{L} \to -\infty \tag{6.16}$$

The general solutions in the neutral and convective limits read:

$$\Delta = \frac{1}{2}\gamma h + C^* h^{-1} \qquad \text{for } L \to -\infty$$

$$\Delta = \frac{A}{1+2A}\gamma h + C^* h^{-(1+A)/A} \qquad \text{for } L \to -0$$

where C^* is the integration constant that can be determined from the initial conditions. The influence of C^* diminishes as the mixed layer grows; under convective conditions, the influence decreases with height to the power -6 ($A = 0.2$), whereas the decrease is somewhat less, to the power -1, in the neutral atmosphere.

In order to derive the equation for the mixed layer height, an expression is needed for the inversion strength. However, even when the influence of the initial conditions of the inversion strength is neglected, the analytical solution to Equation 6.13 is rather unattractive (Gryning & Batchvarova, 1990a). Therefore, the approximation with correct asymptotic limits for neutral and convective conditions is given in Equation 6.17 and will be used in the model:

$$\Delta = \frac{Ah - B\kappa L}{(1+2A)h - 2B\kappa L}\gamma h \qquad (6.17)$$

When the surface heat flux is zero, it follows from Equation 6.14 that $\Delta = \frac{1}{2}\gamma h$, irrespective of the value of B, as can be seen in Figure 6.2a. Originally stratified air has been mixed into the boundary layer without net addition of heat, and therefore the two

hatched regions have equal areas. Figure 6.2b illustrates the encroachment situation, in which the heat flux at the inversion is completely disregarded, corresponding to $A = 0$ and $B = 0$. Then, $\Delta = 0$ and heat supplied from the surface is simply used to fill the original temperature profile. The physically more realistic case for convective conditions where $A = 0.2$, as in Figure 6.2c, results in $\Delta = \frac{A}{1+2A}\gamma h$. Then the boundary layer receives heat both through the interface and from the surface.

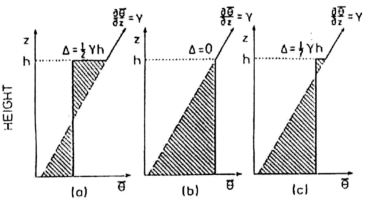

Figure 6.2: The heat budget in the case of (a) mechanical entrainment; (b) entrainment with $A = 0$ and $B = 0$ (encroachment); and (c) convective entrainment with $A = 0.2$.

6.2.5 Mixing Layer Height

To derive a rate equation for h we start from Figure 6.2 where it can be seen that

$$\overline{\theta_{bl}} = \gamma h - \Delta + constant \qquad (6.18)$$

Differentiation of Equation 6.18 with respect to t yields,

$$\left(\frac{d\bar{\theta}}{dt}\right)_{bl} = \left(\gamma - \frac{d\Delta}{dh}\right)\frac{dh}{dt} \tag{6.19}$$

and taking $\frac{d\Delta}{dh}$ from Equation 6.13 and Δ from the approximation of Equation 6.17, substituting into Equation 6.19 leads to:

$$\gamma h\left(\frac{(1+A)h - B\kappa L}{(1+2A)h - 2B\kappa L}\right)\frac{dh}{dt} = \left(\overline{\omega'\theta'}\right)_s - \left(\overline{\omega'\theta'}\right)_h \tag{6.20}$$

Inserting Equation 6.8 into Equation 6.20 leads to the desired differential equation for h (the growth rate of the mixing layer):

$$\left\{\left(\frac{h^2}{(1+2A)h - 2BkL}\right) + \frac{Cu_*^2 T}{\gamma g[(1+A)h - BkL]}\right\}\frac{dh}{dt} = \frac{(w'\theta')_s}{\gamma} \tag{6.21}$$

The relative contributions of mechanical and convective turbulence and the spin-up term to the growth of the boundary layer can be deduced from the left hand side of Equation 6.21. The first term stems from the combined effect of mechanical and convective turbulence, and the second term is due to the spin-up effect.

The contributions from mechanical and convective turbulence are equal when

$$(1+2A)\,h = -2Bk\!L \tag{6.22}$$

The growth of the mixed layer is controlled mainly by convective turbulence when its height h is larger than -2B*k*/(1+2A)* L, and by mechanical turbulence when it is smaller. With the values of A and B, this corresponds to

$$h \approx -1.4L \tag{6.23}$$

By setting $A = 0$, $B = 0$, and $C = 0$, the model reduces to the encroachment model (which deals only with the thermodynamics and neglects turbulent entrainment) for the growth of the mixing layer:

$$\frac{dh}{dt} = \frac{(\omega'\theta')_s}{h\gamma} \tag{6.24}$$

In this study, values of $A = 0.2$, $B = 2.5$, and $C = 8$ were used (after Batchvarova & Gryning, 1991, 1994). Moreover, the model was used with a small modification: a small change was made to the set of equations, in which potential temperature was replaced by virtual potential temperature to include the effects of moisture.

6.3 INITIAL AND BOUNDARY CONDITIONS FOR THE MODEL

Initial values of the boundary layer height, of the thermal gradient above the inversion, and of virtual potential temperature have to be provided for each simulation. These data should be measured at the time of the nocturnal boundary layer breakdown, or in the early morning soon afterwards.

In order to simulate the experiment, heat flux, friction velocity, and temperature must be known as a function of time, and potential temperature gradient as a function of height. Hourly values of surface fluxes and the friction velocity were obtained from eddy-correlation instruments used to construct the energy and momentum fluxes at the surface. These fluxes are important in understanding and analysing the influence of the surface fluxes (as forcings) on the structure of the ABL in the tropics. The average surface fluxes (momentum, heat, and latent heat fluxes) obtained in chapter V are used to prescribe the input energy to the convective boundary layer model.

For heat flux and friction velocity, 10-minute averaged measurements from the sonic measurements presented in Chapter V were used. The potential temperature gradient was derived from the temperature profile as measured by the radiosonde in the early morning before the surface inversion began to break up. The top of the surface temperature is easily identified by the kink in the temperature profile (Chapter IV). The initial values, contained in Table 6.1, were obtained from the composite simultaneous radiosonde ascent taken at 8:00 LT during the TBLE experiments.

Table 6.1: Initial conditions for the boundary layer used to simulate the growth of the mixing layer during the NE-TBLE and the SW-TBLE.

Experiment	H(m)	γ_o (K/km)	θ_s(K)
NE-TBLE	300	4.36	301.75
SW-TBLE	300	3.76	303.625

It is important to note that, in all the analyses throughout this thesis, average values have been computed and compared with average observational aspects. This approach

(composite time evolution) has been chosen, instead of predicting values for individual days, to remove some of the observational noise and day-to-day variability from the results (Fisch *et al.*, 1996).

6.4 MODEL SIMULATIONS OF THE CONVECTIVE BOUNDARY LAYER GROWTH DURING THE NE-TBLE AND SW-TBLE

Using the initial boundary conditions and surface fluxes, the growth of the daytime boundary layer over the tropical site was simulated. The model given in Equation 6.21 was used, with values of empirical constants of 0.2, 2.5, and 8 for *A*, *B*, and *C* respectively. The main results obtained from the simulation are summarized in Tables 6.2 and 6.3 for the NE-TBLE and SW-TBLE respectively.

The hourly values of the growth of the CBL height and virtual potential temperature (θ_v) are shown along with the observed values obtained from the TBLEs, in a series of figures. Figures 6.3 and 6.5 show the CBL simulations for the NE-TBLE and SW-TBLE respectively; continuous lines represent the calculated values and circles represent the observed values. Figures 6.4 and 6.6 show the virtual potential temperature simulations for the NE-TBLE and SW-TBLE respectively; a dashed line represents the computed values and squares represent the observed values.

For the NE-TBLE, the CBL height was underestimated by the model. The model is unable to reproduce the rapid development of the CBL during the early and mid

morning hours (Figure 6.3). The height at 12:00 LT was computed to be 714 m, compared with an observed value of 1800 m, resulting in a lower height achieved in the afternoon. At 16:00 LT the computed height was 1173 m compared with the observed value of 2050 m. The hourly virtual potential temperature was also computed. At 12:00 LT, the computed value was 303.28 K versus an observed value of 305.19 K. At 16:00 LT, the final computed value of the virtual temperature was 305 K (1.6 K less than the observed value). Overall the temperatures computed by the model were lower (Figure 6.4).

The results obtained for the simulation during the SW-TBLE show that CBL heights were 754 m and 1248 m, with differences of 445 m and 650 m compared to observed values, at 12:00 and 16:00 LT respectively (Figure 6.5). The model is unable to reproduce the rapid development during the early and mid morning, similar to the pattern for the NE-TBLE. The value of the virtual potential temperature computed by the model is 1.3 K lower than observed, but at midday the model reproduces the observed temperature reasonably well (Figure 6.6). The difference between the computed and observed value at that time was only 0.84 K.

The comparisons between simulated and observed values show clearly some characteristics of how the growth process occurs. Initially the supplied heat flux is used to heat the layer (a rapid increase in the virtual potential temperature) and to decrease the discontinuity intensity. The layer then begins to grow. In the afternoon, the convective penetration is initiated and the entrainment flux begins to contribute to the CBL growth.

The physical mechanism of the CBL growth is by the dry and hot air entrainment above the top of the inversion, and later by its vertical mixture.

Table 6.2: Numerical simulation (using Equation 6.21) of the CBL height and the virtual potential temperature during the NE-TBLE.

Time (LT)	Mixing-Height (m)	Virtual Potential Temperature (K)
8:00	300	301.75
9:00	327	301.85
10:00	406	302.14
11:00	549	302.67
12:00	714	303.28
13:00	878	303.9
14:00	1030	304.46
15:00	1105	304.74
16:00	1172	304.99
17:00	1252	305.28

Table 6.3: Numerical simulation (using Equation 6.21) of the CBL height and the virtual potential temperature during the SW-TBLE.

Time (LT)	Mixing-Height (m)	Virtual Potential Temperature (K)
8:00	300	303.63
9:00	330	303.72
10:00	419	304.01
11:00	576	304.52
12:00	754	305.1
13:00	932	305.68
14:00	1095	306.2
15:00	1175	306.46
16:00	1248	306.7
17:00	1333	306.98

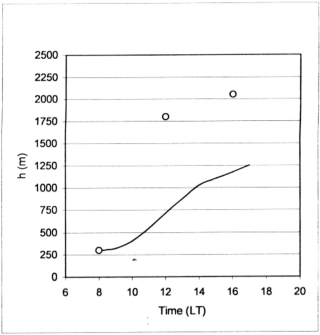

Figure 6.3: Comparison of computed average values (full line) and observations (o) for the mixing height during the NE-TBLE.

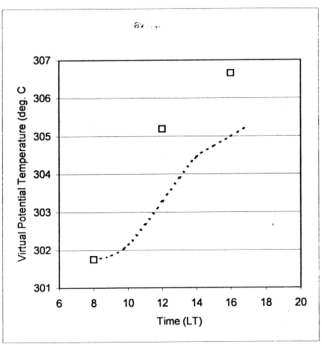

Figure 6.4: Comparison of computed average values (dashed line) and observations (□) for the virtual potential temperature during the NE-TBLE.

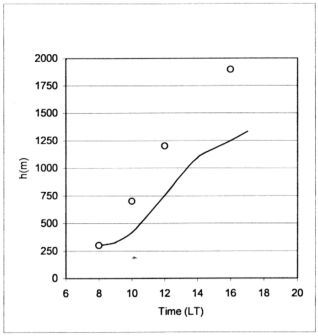

Figure 6.5: Comparison of computed average values (full line) and observations (o) for the mixing height during the SW-TBLE.

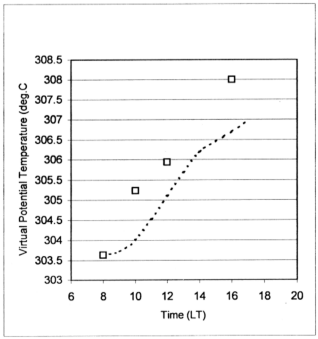

Figure 6.6: Comparison of computed average values (dashed line) and observations (□) for the virtual potential temperature during the SW-TBLE.

The performance of the model was investigated qualitatively by using an even simpler representation of the CBL. The encroachment model has been considered previously for the growth of the mixed layer. For operational use, it is a quick and simple way to calculate the height of the mixed layer. The model is known to perform well under very convective conditions. Encroachment is the situation where the negative heat flux at the inversion base is completely neglected. The heat supplied from the surface is then simply used to fill the original temperature profile.

Using typical data for the TBLEs (from Tables 6.1 and 5.2), Figures 6.7 and 6.8 show simulations of mixed layer height using such an encroachment model (Equation 6.24) and the model presented in Equation 6.21 for which the results have been reported above. The observed values as measured during the TBLEs are also displayed on Figures 6.7 and 6.8. The encroachment model underestimates the mixing layer height, as previously found by Garrett (1992). The model gives lower values than the model of Equation 6.21, and provides an even more severe underestimation of the observed values in both TBLEs. The final height is computed as 996 m (compared to the observed value of 2050 m) during the NE-TBLE (Figure 6.7), and of 1059 m (compared to observed value of 1900 m) during the SW-TBLE (Figure 6.8). The difference is very large and indicates that an additional source of energy is missing from the model. Therefore, the encroachment model fails completely under tropical conditions, showing the importance of mechanical turbulence and the processes operating in the entrainment zone in the tropical setting.

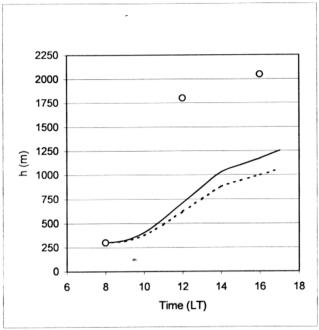

Figure 6.7: Simulation using Equation 6.21 (full line), and the encroachment model of Equation 6.23 (dashed line), of the height of the mixed layer during the NE-TBLE. Observations are shown as circles.

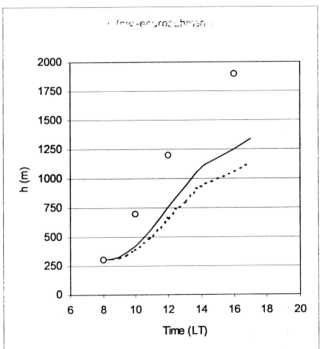

Figure 6.8: Simulation using Equation 6.21 (full line), and the encroachment model of Equation 6.23 (dashed line) of the height of the mixed layer during the SW-TBLE. Observations are shown as circles.

6.5 SUMMARY AND DISCUSSION

A conventional slab model has been used to investigate the ability of numerical models to simulate the growth of the CBL in the tropics. The model was used with a small change having made to the set of equations in which the potential temperature was replaced by the virtual potential temperature in order to include the effects of moisture. The data set collected during the TBLEs was used to verify the model simulations.

Regarding virtual potential temperature, the values computed using the slab model agree rather well with the observed values, giving a difference between the computed and observed values in the order of 1.5 K. The computed value of the virtual temperature was always less than the observed value. The lower value of the temperature computed by the model could be explained by the long time period used by the model to decrease the values of the discontinuity in the virtual temperature at the top of the mixing layer. Only after that is the value of the discontinuity small enough to allow the entrainment fluxes to become significant (Fisch *et al.*, 1996). A similar case was observed and reported by Fisch *et al.* during the RBLII (Forest case). Because of this slow initial increase, the computed value of θ_v is less than the observed value throughout the integration period during the TBLEs.

Regarding mixing height, there is a large difference between the observed and computed mixing heights during both the NE-TBLE and SW-TBLE experiments. For both experiments, this defect is attributed to the slab model being unable to reproduce

the observed rapid development of the convective boundary layer during the morning period. It seems that the ability to simulate the growth of the boundary layer during the afternoon is better. This indicates that there is an additional source of energy missing from the model, and the effect is most pronounced in the morning hours.

The observed CBL heights are higher than the model-predicted CBL height in the hours after sunrise. This may be due to the fact that a well-defined CBL normally begins no earlier than two hours after sunrise (Beyrich, 1995). Moreover, the CBL structure is dominated by nocturnal inversion/stable layer characteristics, whereas the CBL height is dominated by the adiabatic ascent of an air parcel from the surface. This leads to deviations in predicting the CBL height in the morning and in successive hours (Nagar *et al.*, 2001). A similar difficulty was also experienced in modelling the CBL height at Anand, India.

In modelling the convective boundary layer growth in Rondônia, Brazil, over a landscape characterised by humid air, Fisch *et al.* (1996) noticed that the simulated values of the thermal and mechanical contributions to the entrainment flux are almost equal in the early morning. During this time, the mechanical contribution to the entrainment would be expected to be dominant. In contrast, Culf (1992) showed that during the mid-morning period in the semi-arid Sahel, which is characterised by dry air, that the contribution to the entrainment flux from the mechanical turbulence could be ten times greater than the thermal contribution.

These contrasting previous findings indicate that there might be significant underestimation of mechanically generated turbulence in the slab model for humid air conditions. This underestimation is possible as the estimates of the friction velocity from the turbulence measurements by the sonic are known to be rather uncertain, especially when the values of u_* are small (Batchvarova & Gryning, 1991). Larger values of u_* in the model simulations would increase the mechanical contribution to the entrainment flux and increase the rate of the convective boundary layer growth.

Differences between observed and computed CBL heights during the SW-TBLE are smaller compared to those of the NE-TBLE simulation. This is particularly the case at 12:00 LT, when the difference was only 445 m (for the SW-TBLE) compared to 1085 m (for the NE-TBLE). A possible explanation is that the surface fluxes, used as surface forcings to the model, were measured during the SW monsoon (August, 2001). Therefore the measurements were able to represent the actual fluxes to the growth of the CBL better during this season than for those of the NE season.

6.6 CONCLUDING REMARKS

In general terms, the slab model in its current formulation is unable to satisfactorily reproduce the characteristics of the observed convective boundary layer during the TBLEs. There are discrepancies in both the CBL height and the virtual potential temperature profiles. However, the model clearly shows some characteristics of the growth processes and the same trend of the observations, although underestimated, during the morning hours. A poor agreement with observations, especially in the mid

morning is a key issue as several processes can operate to increase the turbulence in the early morning, leading to a more rapid growth of the CBL. This leads toward the necessity of further investigations in the modelling of the tropical CBL. In particular, an additional source of energy is required in the model formulation, and an assessment is needed of the empirical constants used in the model (which represent the mechanical and thermal contribution to the entrainment flux).

The encroachment model simulations indicated even larger differences between the computed and observed values of the mixing layer height than did the slab model. The encroachment model is a better representation of a growth controlled completely by convection. This is not the case in the tropics where the growth of the mixing layer is controlled by both convective and mechanical turbulence. Under such conditions, the encroachment model fails completely to simulate the growth in the tropics. Thus it is not adequate to neglect the heat flux through the top of the boundary layer and the mechanical turbulence, as assumed in the encroachment model. Entrainment through the CBL top is important and contributes to the growth of the layer; therefore, it should be considered in any equation describing the growth of the CBL.